# MARINER 10: MERCURY ATMOSPHERE

A. L. Broadfoot

Kitt Peak National Observatory, Tucson, Arizona 85726

D. E. Shemansky *

University of Michigan, Ann Arbor, Michigan 48105

S. Kumar

Jet Propulsion Laboratory, Pasadena, California 91103

Abstract. Reduction of data from the three Mariner 10 encounters to this date have allowed identification of helium and hydrogen as atmospheric constituents. Subsolar point densities are estimated at 4500 $cm^{-3}$ for He and 8 $cm^{-3}$ for the thermal component of H. A non-thermal component in H with a scale height of $\sim$ 70 km has been observed near the limb off the subsolar point, providing a total apparent number density of 90 $cm^{-3}$. Upper limits on other atmospheric constituents have been reduced an order of magnitude. A very tentative identification of O has been obtained but the uncertainty is large and we require further data reduction for confirmation.

Introduction. Observations in the ultraviolet were made by two spectrometers, in the 300-1700 Å region of the spectrum. One instrument was designed for remote atmospheric sensing of radiation below 950 Å through solar eclipse by the planet (Broadfoot, et al., 1977a). The other instrument was designed for observation of emission at discrete locations in the spectrum (Broadfoot et al., 1977b). The spectral locations were chosen for the observation of $He^+$, He, Ne, Ar, H, O, Xe and C. The spectrometer also included two zero-order channels for broadband integration of the spectrum. We describe here the results obtained to date from the data on three encounters with Mercury.

## 1.0 Airglow Experiment

Atomic hydrogen and helium have been definitely identified as constituents of the Mercury atmosphere, with well defined measurable scale heights. Measurements of helium and hydrogen were made with either discrete steps of the spacecraft scan platform with the solid planet within the instrumental field or with relatively smooth drifts of the planet through the field of view. A number of other programmed observations were also made above the subsolar point. Additional useful data has been obtained during those occasions in which the scan platform pointing was controlled by the television system program. The geometrical distribution of the data as a whole can provide a measure of the global atmospheric distribution, but not without an interpolation process involving comparison with atmospheric models. The necessity for at least some dependence on models for interpretation is due largely to the very low data rates provided by the tenuous condition of the atmosphere. The data obtained above the subsolar point, as explained below, presents the least resistance to interpretation, and is relatively model independent. The observations with the planet within the instrumental field are more difficult to interpret due to the albedo of the surface, and the rapid variations of surface temperature occuring in the region of the terminator. Interpretation of the latter observations requires direct comparison with atmospheric models.

Table I shows the estimated number densities ($N_o$) along with upper limits of the other constituents at the subsolar point.

### 1.1 Helium

The notable feature of the observations above the subsolar point is the apparent determination of the atmospheric altitude distribution by the surface temperature of the planet. Figure 1 shows data obtained at an instrument-planet range of about 25,000 km, in 584 Å radiation, after subtraction of the interplanetary background. The instrumental altitude resolution element is shown in the figure. The smooth curve drawn through the data points is a model exosphere based on the assumption of complete saturation of the surface in He and 100% thermalization of the impacting atoms. The curve is in agreement with the corresponding calculation in the Hartle et al. (1975) model, in which the exosphere extends to the planet surface. The surface temperature in this calculation is 575°K at the subsolar point, with a distribution over the planet approximating the radiative equilibrium calculations by Morrison (1970).

A set of observations across the planet is shown in Figure 2 in comparison with the model convolved with the instrumental function. The solid points representing the model do not include the planet albedo, whereas this quantity is included in the data. The geometry associated with the measurements is shown in the top half of the figure. The signal was integrated for 42 seconds at the position of each mark along the planet centerline. Four sets of data were obtained in the terminator region at ranges of

*Present address: Kitt Peak National Observatory, Tucson, Arizona 85726.

TABLE I. ESTIMATED NUMBER DENSITIES AND UPPER LIMITS AT THE SURFACE SUBSOLAR POINT OF MERCURY
Measurements from Mariner 10 UVS--Mercury I, III Encounters

| Emitter | Channel (Å) | Brightness (Rayleighs) [a] | g (ph $sec^{-1}$) | $N_o$ ($cm^{-3}$) [b] | P (mb) [c] |
|---|---|---|---|---|---|
| He | 584 | 70 [1] | 6.8 - 5 | 4.5 + 3 | 3.6 - 13 [1] |
| Ne | 740 | 4.1 [3] | 5.1 - 8 | 1.5 + 6 | 1.2 - 10 [3] |
| Ar | 869 | 6.6 [3] | 4.2 - 7 | 8.7 + 5 | 6.9 - 11 [3] |
| Ar | 1048 | 36 [3] | 1.4 - 6 | 1.4 + 6 | 1.1 - 10 [3] |
| H | 1216 | 70,720 [1,4] | 1.5 - 2 | 8.0,82 [4] | |
| O | 1304 | 63 [2] | 1.3 - 4 | 7.1 + 3 | 5.6 - 13 [2] |
| Background | 1480 | | | | |
| C | 1657 | 25 [3] | 1.4 - 3 | 1.9 + 2 | 1.5 - 14 [3] |

*a.* Estimates at 60 km altitude.
*b.* Ground level.
*c.* T = 575°K; from He scale height.
*1.* Measured quantities with well defined scale height.
*2.* Measured quantity but with very uncertain identification of scale height.
*3.* Upper limits.
*4.* Thermal and non-thermal components respectively; see text.

88,000 km and 27,000 km incoming, and 89,000 km and 24,600 km outgoing. All four sets of observations are consistent in the detail of the observed variations in Figure 2. As the figure illustrates, we find a significant deviation from the model in the terminator region and across the darkside of the planet. The signal predicted by the model at the terminator with normalization to the data at the subsolar point is an order of magnitude greater than observation.

It has been clearly pointed out by Hartle et al. (1975) that the model calculations of surface number density in the immediate region of the terminator are somewhat uncertain due to discrepancy of the temperature variation used in the model compared to more accurate computed temperature estimates (Chase et al., 1976). Thus there is a question as to whether or not the discrepancy with the model is confined only to the terminator region and results entirely from a crude approximation to the temperature variation in this region. In our judgment the discrepancy is of a more fundamental nature.* The data in the terminator region suggests significant scale height differences with the 1, indicated by tangent lines A and B in Figure 2, in addition to the differences in relative magnitude. Since surface temperature is the controlling factor and the source and sink functions are not important in the model calculation, there appears to be little one can do but conclude that the assumptions going into the calculation are not valid for Mercury.

The fraction of the subsolar surface density having escape velocity is about $2 \times 10^{-3}$. Based on the measured global distribution, the total loss rate of thermal escape for He is estimated to be $3 \times 10^{23}$ $sec^{-1}$. Assuming the source to be the solar wind, this represents a collection efficiency of $He^{++}$ of $\sim 3 \times 10^{-3}$. The photoionization rate is $\sim 1.3 \times 10^{23}$ $sec^{-1}$. If we apply the Banks et al. (1970) value for the escape factor, the estimated loss rate due to photoionization is $\sim 1 \times 10^{22}$ $sec^{-1}$. The collection rate of He from the interstellar medium is estimated at $\sim 2 \times 10^{21}$ $sec^{-1}$, based on the Mariner 10 UV airglow spectrometer data (Ajello et al., 1976).

Model calculations of the He atmosphere are proceeding with the purpose of determining the nature of the interaction with the surface.

### 1.2 Hydrogen

Figure 3 shows the altitude distribution of H above the subsolar point as observed at a planet-instrument range of $\sim$ 88,000 km. The distribution appears to be approximately thermal, apart from the statistically significant structure apparent in the figure. The curves shown in the figure are model exosphere calculations at the indicated base temperatures. A best fit appears to be in the region of 420°K. It is not clear that the temperature divergence with the He distribution is significant. The H data at 1216 Å have a larger statistical uncertainty due to subtraction of 253 R of interstellar background. As shown in Table I, the estimated number density at the surface due to this component is 8 $cm^{-3}$. This hot distribution suggests that some fraction of the H atoms impacting the surface do not react chemically and have a collision time long enough to thermalize.

Observations at higher resolution in altitude at a range of $\sim$ 25,000 km reveal an abrupt change in scale height at about 300 km altitude above the limb where the distribution changes from a

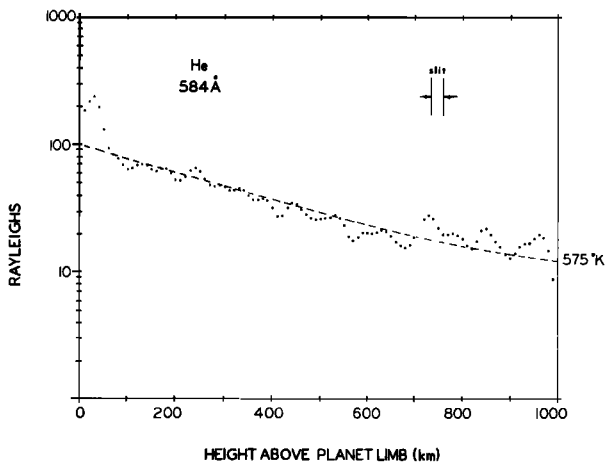


Figure 1. Observations of 584 Å He above the subsolar point at Mercury I encounter.
*Notes:* The altitude is given in km above the limb. Plotted points are smoothed data obtained at a planet-instrument range of $\sim$ 25,000 km.

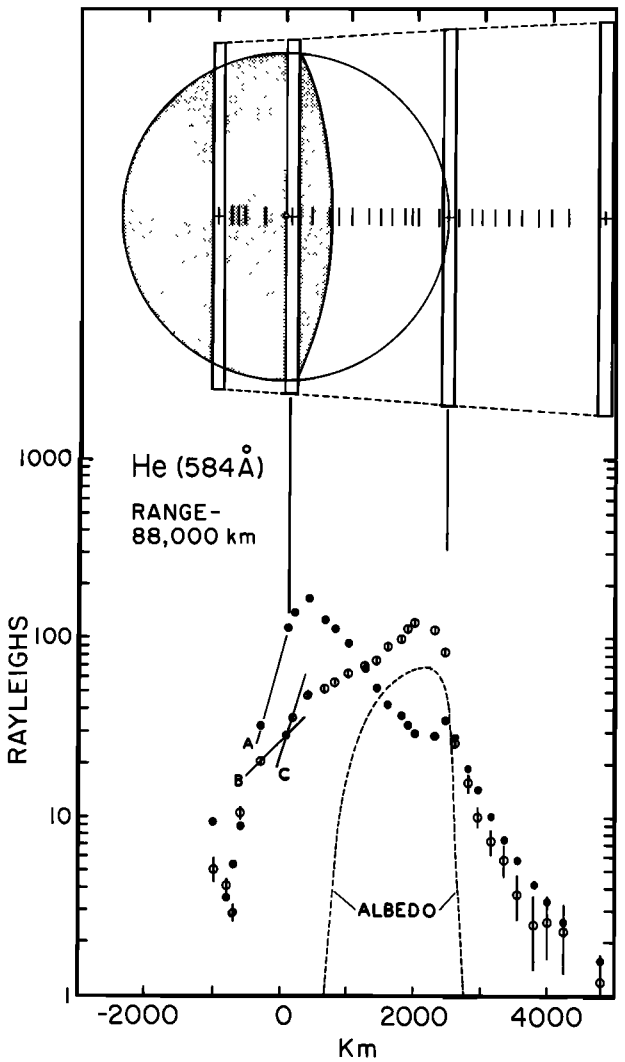


Figure 2. Observations of 584 Å He across Mercury at Encounter III.

1900 km scale height to a 70 km scale height extending down to the surface. The apparent total H number density at the surface is 90 $cm^{-3}$. Apart from the calculated exospheric H distribution above the subsolar point shown in Figure 3, no attempt has yet been made to model the physical chemistry required to explain the remarkable near-limb behavior.

Observations across the terminator onto the dark side of the planet do not provide measurable scale heights in H. Bright reflected 1216 Å radiation from the sun side of the terminator prevents detection of a small scale height in the immediate region of the shadow. However, emission is observed from a component with scale height too large to be measurable with the dynamic range provided by the shadow height. This hot component provides an estimated 25 $cm^{-3}$ surface density at the terminator.

If one assumes that the dominent source of H is photolysis of an $H_2O$ atmosphere and is responsible for the small scale height at the limb, we would require $[H_2O] \simeq 2 \times 10^6$ $cm^{-3}$ at the subsolar point. In this case, the total loss rate of H would be $\sim 10^{24}$ $sec^{-1}$. This would require a solar wind capture efficiency of $6 \times 10^{-4}$, about a factor of 5 less than the corresponding number for $H_e$.

### 1.3 Other Constituents

Data obtained from encounter III indicated a measurable signal in the 1304 Å channel attributed to atmospheric emission. Although the data appear to be statistically significant, the signal to noise ratio is low and a scale height has not been identified. The estimated number density, $[O] = 7 \times 10^3$ $cm^{-3}$ (Table I), at the subsolar point is thus very uncertain and requires confirmation with further data reduction.

Upper limits for the other possible constituents are given in Table I. These values are an order of magnitude lower than those obtained in the preliminary analysis (Broadfoot et al., 1974).

## 2.0 Occultation Experiment

Observation of the atmosphere in absorption in the 300-950 Å region provides a measure of the total atmospheric content since the majority of gases have large measurable cross-sections. The solar flux in this experiment was measured at 470 Å, 740 Å, 810 Å and 890 Å with bandwidths of 75 Å.

No measurable absorption was obtained in any of the channels on eclipse of the sun by the planet (cf. Broadfoot et al., 1974). We estimate an upper limit of 3% absorption at an altitude of 8 km. The number density limits at the terminator are given in Table II. The calculated limits are based on a rough approximation to a model exosphere, taking into account the temperature variation across the terminator.

## 3.0 Discussion

The observed He atmosphere above the subsolar point corresponds to an exosphere with base temperature 575°K. The temperature corresponds to the value obtained in the Morrison radiative equilibrium calculations. The distribution above the subsolar point is reasonably model independent since the surface temperature is uniform over a

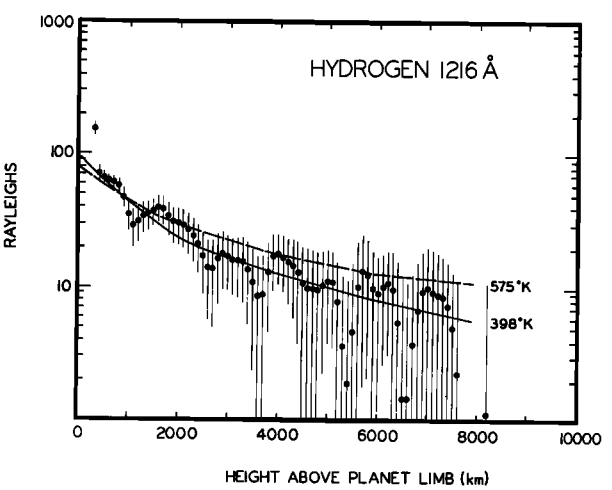


Figure 3. Observations of 1216 Å H above the subsolar point at Mercury I encounter.

TABLE II. MARINER 10 OCCULTATION EXPERIMENT UPPER LIMITS OF MERCURY TERMINATOR NUMBER DENSITY

| | $\sigma \times 10^{17}$ $cm^2$ | $N_o \ell \times 10^{-15}$ $cm^{-2}$ | $N_o \times 10^{-7}$ $cm^{-3}$ |
|---|---|---|---|
| He | 0.8 | 3.7 | 2.6 |
| Ar | 3.5 | 0.9 | 3.1 |
| O | 1.2 | 2.5 | 4.2 |
| $CO_2$ | 7.4 | 0.4 | 1.6 |
| $H_2O$ | 3.6 | 0.8 | 1.5 |
| $O_2$ | 3.5 | 0.9 | 2.5 |
| $N_2$ | 3.3 | 0.9 | 2.3 |
| $H_2$ | 1.0 | 2.9 | 1.4 |

wide surrounding area. It is thus possible to find agreement with the model on the sunside, and disagreement with the darkside observations. The nature of the divergence with the model calculations suggests that the problem lies with the assumptions concerning the interaction of atmospheric He with the surface. The effect of inefficient energy transfer to the impacting He as well as source distribution is presently being examined with our model programs. At this point, we cannot add to the discussion concerning the source of atmospheric He (cf. Kumar, 1976).

Model calculations of possible sources of H compatible with the present observations are at a more primitive stage. Photolysis of an $H_2O$ atmosphere appears to be a strong possibility (Thomas, 1974, Cadenhead and Buergel, 1973), but it is not at all clear, without detailed model calculations, that this is compatible with the observations. We have concluded that it is essential to compare the data with models convolved with the known instrumental function in order to avoid misinterpretation.

Acknowledgment. This work was sponsored by Kitt Peak National Observatory and supported by Jet Propulsion Laboratory, California Institute of Technology, under NASA Contract NAS 7-100.

*Note added in proof: One of the referees has suggested that the disagreement of the He model with observation may be due to the fact that the approximation to the Chase et al. surface temperature distribution was not sufficiently accurate. We have recalculated the He atmosphere using the same method outlined above, with the Chase et al. surface temperature distribution. This has a negligible effect on the predicted relative signal rates at the morning terminator. The new evening terminator predicted rates are lower than those shown in Figure 2 by roughly 25% due to a relatively higher temperature in the immediate dark side region. Although the relative surface number density in the region of peak signal rates near the terminator is reduced from $N/N_o \simeq 200$ in the case shown in Figure 2, to $N/N_o \simeq 125$ in the new model, the increased scale height tends to mask the change in surface density in the predicted signal; the instrument provides a direct measure of atomic abundance, not surface number density.

Our conclusion, therefore, remains the same. Surface temperature distribution appears to be a very unlikely source for the discrepancy. The errors in temperature we would have to attribute to the Chase et al. work are unacceptably large. It would be necessary to raise the temperature of the dark side of the planet as a whole, substantially, to obtain agreement of model and data.

## References

Ajello, J. M., S. Kumar, and A. L. Broadfoot, Mariner 10 ultraviolet experiment: Observations of the interstellar wind, Eos Trans. AGU, 57, 280, 1976.

Banks, P. M., H. E. Johnson, and W. I. Axford, The atmosphere of Mercury, Comments Astrophys. Space Phys., 2, 214, 1970.

Broadfoot, A. L., S. Kumar, M. J. S. Belton, and M. B. McElroy, Mercury's atmosphere from Mariner 10: Preliminary results, Science, 185, 166, 1974.

Broadfoot, A. L., S. S. Clapp, and F. E. Stuart, Mariner 10 ultraviolet spectrometer: Occultation experiment, Space Sci. Inst., 3, XX, 1977a.

Broadfoot, A. L., S. S. Clapp, and F. E. Stuart, Mariner 10 ultraviolet spectrometer: Airglow experiment, Space Sci. Inst., 3, XX, 1977b.

Cadenhead, D. A., W. G. Buergel, Science, 180, 1166, 1973.

Chase, S. C., Jr., E. D. Miner, D. Morrison, G. Münch, and G. Neugebauer, Mariner 10 infrared radiometer results: Temperatures and thermal properties of the surface of Mercury, Icarus, 28, 565, 1976.

Hartle, R. E., S. A. Curtis, and G. E. Thomas, Mercury's helium exosphere, J. Geophys. Res., 80, 3689, 1975.

Kumar, S., Mercury's atmosphere: A perspective after Mariner 10, Icarus, 28, 579, 1976.

Morrison, D., Thermophysics of the planet Mercury, Space Sci. Rev., 11, 271, 1970.

Thomas, G. E., Mercury: Does its atmosphere contain water?, Science, 183, 1197, 1974.

(Received May 17, 1976;
revised July 15, 1976;
accepted August 5, 1976.)